

ANTIBACTERIAL ACTIVITY OF SILVER NANOPARTICLES SYNTHESIZED BY HYDROTHERMAL TECHNIQUE

Shireen Taily Abduljabbar^{1,*}, Tariq Abdul-Hameed Abbas¹

¹Department of Physics, College of Science, Salahaddin University-Erbil, Kurdistan Region, Iraq

*Corresponding author email: Shirin.Abduljabar@epu.edu.iq

Received: 6 Feb 2025 Accepted: 24 Feb 2025 Published: 7 Apr 2025

<https://doi.org/10.25271/sjuoz.2025.13.2.1476>

ABSTRACT:

In this work, Ag NPs were synthesized via a hydrothermal method using silver nitrate (AgNO_3) as precursor material. The impact of PVP concentration on the particle size distribution and surface morphology of Ag NPs in the hydrothermal reaction was studied. The obtained Ag NPs were characterized by UV-Vis, XRD, FESEM, and FTIR measurements. The calculated values of E_g from the absorption peaks of the UV/Vis- spectra were found to be increased from 1.70 eV to 1.87 eV with increasing the concentration of PVP from 0.2 mol/L to 0.5 mol/L. XRD measurements revealed that the Ag NPs are highly crystalline. The FESEM observation results indicated that the optimized synthesized Ag NPs are spherical with an average size of 140 nm. The FTIR results confirmed the Ag NPs formation with presence of several functional groups in Ag NP and pure PVP. The study evaluated the antibacterial activity of Ag NPs based on the diameter of the inhibition zone in the agar well diffusion method. The results indicated that the characteristics and antibacterial activity of Ag NPs could be optimized by altering the concentration of PVP used as a stabilizer. The Ag NPs synthesized without the addition of PVP showed antibacterial activity on both gram-negative bacterium *Escherichia coli* (11 to 12) mm and gram-positive bacterium *Staphylococcus aureus* (12 to 13) mm, meanwhile with using PVP, there is no inhibitory activity towards gram-negative bacteria but showed antibacterial activity on gram-positive (25) mm. The stability of Ag NPs has been investigated by measuring the absorption spectrum of the PVP-Ag NPs, which was found to be stable for nearly 3 months. Synthesis of stable Ag NPs is necessary for later use in the required application.

KEYWORDS: Silver Nanoparticles, Hydrothermal Technique, Polyvinylpyrrolidone Stabilizer, Size Control, Antibacterial Activity

1. INTRODUCTION

Nanoparticles (NPs) can be formed of a variety of materials, including metals, ceramics, polymers, and biological components (Khan *et al.*, 2019). The presence of materials at the nanoscale affords them various advantages and unique properties derived from the properties of materials in standard measurements, the most prominent of which is their small size and high surface-to-volume ratio (Altammar, 2023). It is well known that reducing a body's size increases its susceptibility to the behavior of its fundamental constituents (atoms and particles), resulting in properties that differ from those of conventionally measured objects, such as alterations in physical properties (Wang *et al.*, 2023). In contrast with normal inorganic materials, inorganic nanomaterials have different characteristics related to their sizes at the nanoscale, which may appear as surface effects, size effects, macroscopic quantum tunneling effects, and quantum confinement effects, which provide extensive applications across various fields (Eker *et al.*, 2024; Esmael, 2024).

NPs have attracted significant interest in several fields, such as medicine, electronics, energy, and environmental research, according to their extensive applications and prospective advantages. Silver is a noble metal with enormous deposits and excellent physical properties (Duman *et al.*, 2024). Silver contains excellent flexibility, electrical and thermal conductivity, and can be used widely in electronic and electrical devices, photosensitive materials, chemical substances, and various other areas. The ongoing advancement of nanotechnology has led to the broad development and application of nano-silver due to its excellent electrical conductivity, thermal conductivity, antibacterial properties, optical properties, and other unique characteristics (Cheng *et al.*, 2021; Ghadiri *et al.*, 2023; Yatem & Rammoo, 2023). Ag NPs have unique chemical, biological,

and physical properties. It is commonly used in several kinds of fields, including electronics, biosensors, medicine, environmental remediation, and antibacterial packaging. One of the most important characteristics of Ag NPs is their antibacterial activity. Ag NPs are widely known for their inhibitory impact on common frequent bacteria for medical and manufacturing processes (More *et al.*, 2023; Obaidallah & Ahmed, 2023). Ag NPs are the most effective nanomaterials in the fight against harmful microorganisms (Dakal *et al.*, 2016). At low concentrations, silver is known to be non-toxic and safe for human health, in contrast to other metallic nanoparticles (Ahmad, 2022; Ivlieva *et al.*, 2022). Ag ions are extremely toxic to bacteria. The characteristic that gives Ag NPs their unique behavior in this respect is their larger surface area when compared to the bulk form of silver (Neto *et al.*, 2023). The tiny size of these particles enables their penetration into bacterial and fungal cells, leading to their elimination. Ag NPs are utilized in various medical and healthcare products, including surgical instruments, dressings for injuries, and antimicrobial coatings for medical devices (Ferreira *et al.*, 2023).

Nanoparticles can be manufactured using numerous approaches, which are generally classified into three categories: chemical, physical, and biological methods (Yaqoob *et al.*, 2020). In summary, there are a number of drawbacks to the physical synthesis of Ag NPs, such as high energy consumption, a slow rate of production, and complex operation. The biologically produced synthesis method for nano-silver is an economical and environmentally friendly technique; however, it poses challenges for large-scale production of nanoparticles. Compared to other procedures, the chemical technique is recognized as an efficient, convenient, and easily controllable approach. A reducing agent transforms silver ions into Ag NPs during the chemical reduction process (Abbas *et al.*, 2024). The reaction may occur in solution

* Corresponding author

This is an open access under a CC BY-NC-SA 4.0 license (<https://creativecommons.org/licenses/by-nc-sa/4.0/>)

or on a solid substrate, with the dimensions and form of the resulting nanoparticles modifiable by altering reaction parameters such as time, temperature, and amount of reactant. However, a concern associated with the chemical reduction process is the tendency for nanoparticles to cluster during production or storage, potentially resulting in the loss of their distinctive properties. The hydrothermal synthesis method is a widely used chemical approach for synthesizing metal NPs at high temperatures and pressures utilizing a solvent. This hydrothermal technique has been successfully used to produce a wide variety of metal nanoparticles (Li *et al.*, 2016). The hydrothermal synthesis technique is regarded one of the most promising methods to generating nanoparticles. This technique has been extensively applied for various chemical procedures such as materials preparation, crystal formation, and waste management. The hydrothermal process is defined as conducting chemical reactions in a solvent within sealed vessels, where the solvent's temperature can be elevated to near its critical point while maintaining autogenous pressures through heating (Feng & Li, 2017). When water is used as a solvent, the process is known as "hydrothermal". Particle preparation can be changed by altering elements, including precursor mixture concentration, the temperature of the reaction, and reaction time (Khizir & Abbas, 2021; Liu *et al.*, 2024). The reaction medium is critical because the solvent's properties can be altered by modifying the kind and volume ratio of the solvent employed (Slewa *et al.*, 2019).

Bandura and colleagues reported that preparation of Ag NPs by hydrothermal method for high-throughput biosensing applications with an average particle size of 45 nm was conducted using silver nitrate as a precursor, ethylene glycol, and PVP as a stabilizing agent. Changes to particle shape and size were achieved by variation in the PVP: Ag molar ratio of the

precursor mixture (Bamiduro *et al.*, 2018). Tooklang and colleagues reported synthesizing Ag NPs by hydrothermal method for improved antimicrobial properties using an aqueous solution of silver nitrate (AgNO_3), glucose, NaCl and PVP as a stabilizing agent, resulting in spherical particles with a size of 120 nm (Tooklang *et al.*, 2024).

In this work, various types of Ag NPs as well as surface modifications of nanomaterials were synthesized by using hydrothermal route from AgNO_3 powder as a target process, using deionized water as a solvent, and PVP serves as a capping agent to regulate shape, thus raising the chemical activity on the surface of the membrane.

The effects of PVP concentrations on the structural, morphological, and optical properties of the produced nanostructures were studied. The antibacterial efficacy of the synthesized nanoparticles was assessed against several human pathogenic bacteria using the agar well-diffusing assay. Further, the antibacterial activity results of the prepared nanoparticles were compared with the antibacterial activity of ampicillin as a reference antibiotic drug.

2. Experimental

Hydrothermal Process:

The traditional method for producing metal nanoparticles by hydrothermal technique, such as silver (Ag), includes reducing Ag^+ ions in a liquid media like water, usually with the addition of a stabilizing substance such as PVP. The hydrothermal process normally includes a Teflon-lined stainless-steel autoclave, a magnetic stirrer, and an electric oven quartz tube furnace. Figure 1 depicts a schematic representation of the hydrothermal method and production mechanism for the synthesis of Ag NP

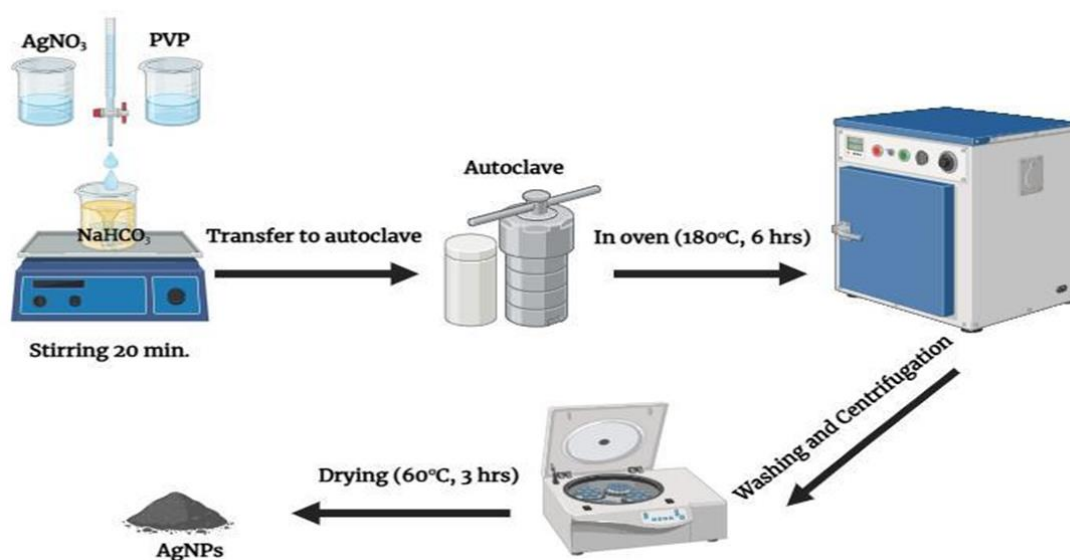


Figure 1: Schematic diagram displaying the steps for hydrothermal synthesis of Ag NPs

Materials:

The following materials and solvents were used in the experiments:

The materials and solvents employed in this research, as well as the description, included as follows: silver nitrate (AgNO_3) (BIOCHEM), poly (N-vinylpyrrolidone) (PVP-K30, BIOCHEM), sodium bicarbonate (NaHCO_3) (BIOCHEM), deionized water, and ethanol (Hongwell).

Hydrothermal Method for Synthesizing Ag Nps:

In a hydrothermal procedure, 20 mL of deionized water was used to dissolve 0.2 mol/L AgNO_3 . In a separate container, PVP was dissolved in 30 mL of deionized water at varying concentrations. Both solutions were added dropwise to a solution of NaHCO_3 , which was prepared by dissolving 0.05 mol/L NaHCO_3 in 20 mL of deionized water. The final product was subjected to continuous magnetic stirring at room temperature for 20 minutes to achieve a homogeneous mixture of the reaction. Then 70 ml of the mixture were transferred into a 100 mL Teflon-lined stainless-steel autoclave and heated to a fixed temperature of 180 °C for 6 hours. After the heating period, the autoclave was

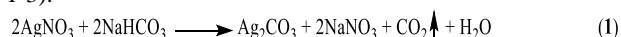
allowed to cool to room temperature naturally. Subsequently, the solutions were centrifuged multiple times using water and ethanol to remove impurities. Finally, the samples were dried in an electric oven (quartz tube furnace) at 60 °C for 2 to 3 hours to

obtain the silver nanoparticle powder. Various concentration samples were prepared, labeled as N₀, N₁, N₂, N₃, and N₄, corresponding to PVP concentrations of 0, 0.2, 0.3, 0.4, and 0.5 mol/L, respectively, as indicated in Table 1.

Table 1: The chemicals and solvents used in the hydrothermal procedure for synthesis Ag NPs in this work

Sample	AgNO ₃ Concentration (mol/L)	NaHCO ₃ Concentration (mol/L)	PVP Concentration (mol/L)	Temperature (°C)	Time (h)
N ₀	0.2	0.05	0	180	6
N ₁	0.2	0.05	0.2	180	6
N ₂	0.2	0.05	0.3	180	6
N ₃	0.2	0.05	0.4	180	6
N ₄	0.2	0.05	0.5	180	6

The chemical reaction equations describing the formation mechanism of the synthesized Ag NPs are provided below (Eqs. 1-3):



As the growth method, the new silver atoms generated gradually increase, and when the concentration of silver atoms reaches a critical supersaturated concentration, nucleation occurs, and the nuclei formed continue to grow into Ag NPs (Liu *et al.*, 2024).

Characterizations:

The synthesized silver nanoparticles (Ag NPs) were characterized, and the optimal sample was selected for antibacterial activity assessment. The main physical and chemical properties of the Ag NPs, including shape, size, surface plasmon resonance, surface charge, and stability, have been measured and analyzed for their characterization.

UV-Vis spectroscopy (Model Shimadzu 1900i, Japan) has been used to investigate the optical properties of the synthesized Ag NPs; the crystalline structure of the synthesized samples was investigated by X-ray crystallography (XRD) using a diffractometer (Bruker D8, Germany) with Cu K α ($\lambda = 1.5406 \text{ \AA}$) radiation (30 kV, 30 mA). Field-emission scanning electron

microscopy (FESEM) was used to record the morphological features of the synthesized samples using (Tescan Mira3, Czech Republic). The Fourier-transform infrared spectrometer (FTIR) technique (Model Shimadzu Corporation, Japan) in the range of 4000-400 cm⁻¹ with a resolution of 4 cm⁻¹ was used to observe the surface functional groups.

Then after, the antibacterial activity of the optimally synthesized Ag NPs was evaluated against bacterial strains (*Entamoeba coli* as Gram-negative bacteria and *Staphylococcus aureus* as Gram-positive bacteria) using the agar-well diffusion technique.

3. RESULTS AND DISCUSSIONS

UV-Vis Absorption Spectra :

The optical characteristics, as well as the stability of the acquired samples, were assessed using UV-VIS spectroscopy. For structural characterization of Ag NPs, one of the most popular methods is UV-visible spectroscopy. The technique is responsive to the surface plasmon excitation of Ag NPs, shown by an absorption peak, and assesses the stability and properties of Ag NPs. The absorption spectrum of the synthesized Ag NPs is recorded as a result of wavelength within the range of 200 to 800 nm.

Figure 2 depicts the absorption UV-vis spectra of Ag NPs prepared without PVP (sample N₀) and those prepared under various concentrations of PVP for the samples (0.2, 0.3, 0.4, 0.5 mol/L) after 15 h of reaction time over the range of (200-800) nm wavelength

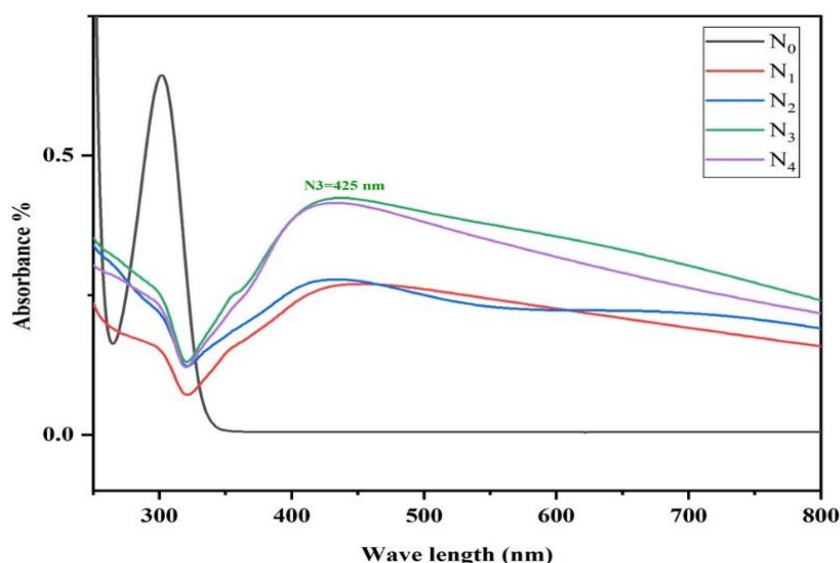


Figure 2: The absorption spectra of Ag NPs synthesized without PVP (sample N₀) and those synthesized with various amounts of PVP (0.2, 0.3, 0.4, 0.5 mol/L) for samples N₁, N₂, N₃, and N₄, respectively

The results of Figure 2, indicated that the absorption spectrum is characterized by a broad absorption band that appears between about (400 to 500) nm with a maximum intensity around 425 nm, which is the surface plasmon resonance (SPR) band of Ag NPs, indicating the production of Ag NPs having a wide size distribution. The peak at a position of about 425 nm is indicate to the SPR peak of spherical Ag NPs, confirming the generation of small Ag NPs in this system with a nanosized. Addition of PVP in the synthesizing process of Ag NPs influences the location of the SPR peak and thus the dimension of the produced NPs. This result is also confirmed by FESEM images.

Without the PVP sample (N₀), no absorption peak was observed in the visible region, indicating that PVP acts as a reducing agent as well as a capping agent for the formation of Ag NPs under hydrothermal conditions. However, the size of the synthesized Ag NPs is observed by the shift of the absorption peak towards a longer or shorter wavelength. The intensity of the absorption peak is directly proportional to the concentration of Ag NPs in colloidal solution. The results revealed that with increasing PVP concentration, synthesized Ag NPs exhibited higher intensity peak absorption with a lower SPR peak (blue shift). The smaller size of the synthesized Ag NPs with higher peak intensity is observed for the concertation of 0.4 mol/L of PVP sample (N₃). Moreover, the sample at a higher concentration of 0.5 mol/L of PVP sample (N₄) the SPR peak shifted to a higher wavelength (red shift). This proved that the production of Ag NPs

was restricted by a high PVP concentration. The significant amount of stabilizer causes the creation of a shield, preventing the detection of nanostructures. Furthermore, the significant amount of stabilizer can prevent Ag NPs from interacting with other compounds due to being entangled in the dense network of the stabilizer. This describe the low strength of the SPR peak at high PVP concentrations. It could deduce that a specific amount of PVP as a stabilizer can yield the best Ag NPs sample. The UV-Vis absorption spectra of all synthesized Ag NPs confirm the XRD and FESEM results.

Further, the optical band gap energy of the prepared samples was determined. Figure 3, shows the Tauc plot ($\alpha h\nu$)² vs. energy (hν) of Ag NPs prepared at various amounts of PVP (0.2, 0.3, 0.4, and 0.5) mol/L for samples N₁, N₂, N₃, and N₄, respectively. The intercept of the linear part of the plot on the energy axis provided the values of optical band gap energy (E_g) of the Ag NPs. The E_g obtained were (1.70, 1.74, 1.78, and 1.87) eV corresponding the samples N₁, N₂, N₃, and N₄ respectively, which are the indication of the formation of Ag NPs. The increase in the band gap energy values with increasing the concentration of PVP is due to the decrease in particles size of Ag NPs, the result which consist with the blue shift of SPR absorption UV-vis spectra shown in figure 2 above. The determined values of band gap energy are in agreement with a previous reported paper (Jalal, 2024).

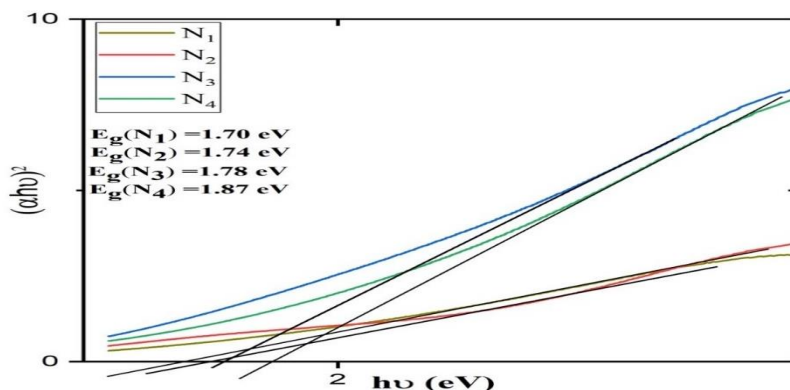


Figure 3: The optical band gap energy of the Ag NPs synthesized at various amounts of PVP (0.2, 0.3, 0.4, and 0.5 mol/L) for samples N₁, N₂, N₃, and N₄, respectively.

XRD Analysis:

X-ray diffraction is a very important method for studying the properties, crystallization, and structure of nanostructures. The crystalline nature of the synthesized Ag NPs was identified by X-ray crystallography. To determine the role of PVP, the XRD

peaks associated with Ag NP production at various PVP concentrations were studied. Figure 4, shows a crystalline form for the obtained Ag NPs synthesized without PVP and those synthesized under various concentrations of PVP (0.2, 0.3, 0.4, 0.5 mol/L).

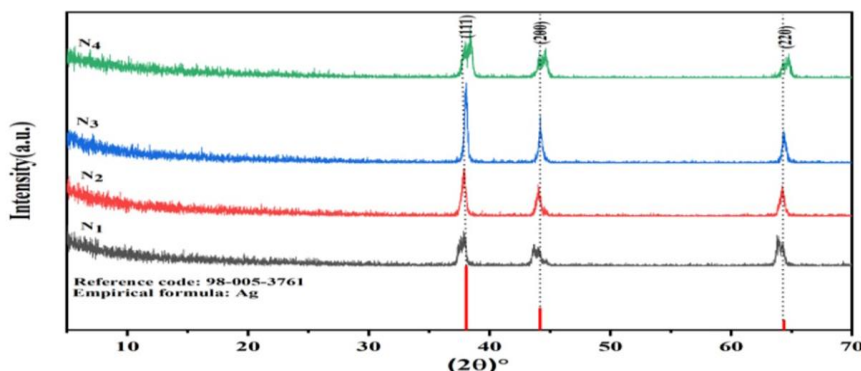


Figure 4: The XRD patterns of the Ag NPs synthesized at various amounts of PVP (0.2, 0.3, 0.4, and 0.5 mol/L) for samples N₁, N₂, N₃, and N₄, respectively

The highest peaks obtained at the positions $(2\theta) = 38.04^\circ$, 44.18° , and 64.37° for all the samples are correlated to the (111), (200), and (220) planes, respectively. The three peaks observed are associated with a face-centered cubic of structure Ag NPs. These products confirmed that Ag NPs were obtained with a cubic crystal system, which is the most common type of silver structure. However, low crystallinity, along without PVP is observed for the synthesized Ag NPs. Meanwhile, the diffraction peaks with PVP are quite sharp, indicating that the Ag NPs result has strong crystallization characteristics as the PVP concentration increases. More crystallinity of the Ag NPs with sharper and narrower diffraction peaks was obtained for sample N_3 at the PVP concentration of 0.4 mol/L, the results of which are quite consistent with FESEM and optical results.

FESEM Analysis:

The morphological information of all prepared Ag NP samples and their micrographs were obtained by FESEM. Also, FESEM gives information about the shape and particle size distribution. The nano silver particle distribution is clearly observed in the FESEM images. The effect of PVP on the formation and characteristics of the product Ag NPs was investigated by preparing precursor mixtures containing different PVP: Ag molar ratios. Figure 5, illustrates the FESEM images of the Ag NPs prepared without PVP and those with using different PVP concentrations.

The image showed without adding (PVP), the particles appear in different and irregular sizes and shapes with a rough surface, Figure 5, (N_0). Without adding of PVP, which is the Ag

NPs rapidly settled due to their substantial particle size, resulting in no formation of nano silver and hence no absorption peak seen near 400 nm (see Figure 2). When (PVP) is added, particles are started to form in nano-sized with some clusters, Figure 5 (N_1) exhibits an average size of particles of 250 nm. As the concentration of PVP increases, the particles turn into regular shapes and are uniformly distributed, Figure 5 (N_2) having an average particle size of nearly 175 nm.

The optimal image of the sample created at 0.4 mol/L of PVP, Figure 5 (N_3), reveals a smooth surface morphology with the dimensions of the grown Ag NPs in the narrow nanoscale range and almost all spherical in shape with some triangle, pentagonal and hexagonal surface, these particles possess a diameter between 50 and 250 nm, average size (mean diameters) of 140 nm, which aligns with the narrow SPR peak observed in the UV-VIS absorption spectra. This size with spherical shape is suitable for biological applications, such as antibacterial activity.

With more increasing of PVP amount to 0.5 mole/L, larger Ag NPs were again produced, Figure 5 (N_4), with an average particle size of 145 nm. Furthermore, an excessive quantity of the stabilizer may inhibit nanoparticle interactions with other substances due to entrapment inside the dense stabilizer network. Also, particle size distribution has been estimated from the FESEM images and was observed to vary with PVP content. The features of Ag NPs can be optimized by adjusting the levels of PVP. As shown in Figure 5, there is a connection exists between the growth of steady PVP concentration and the transformation of Ag NPs to small nanosphere shapes.

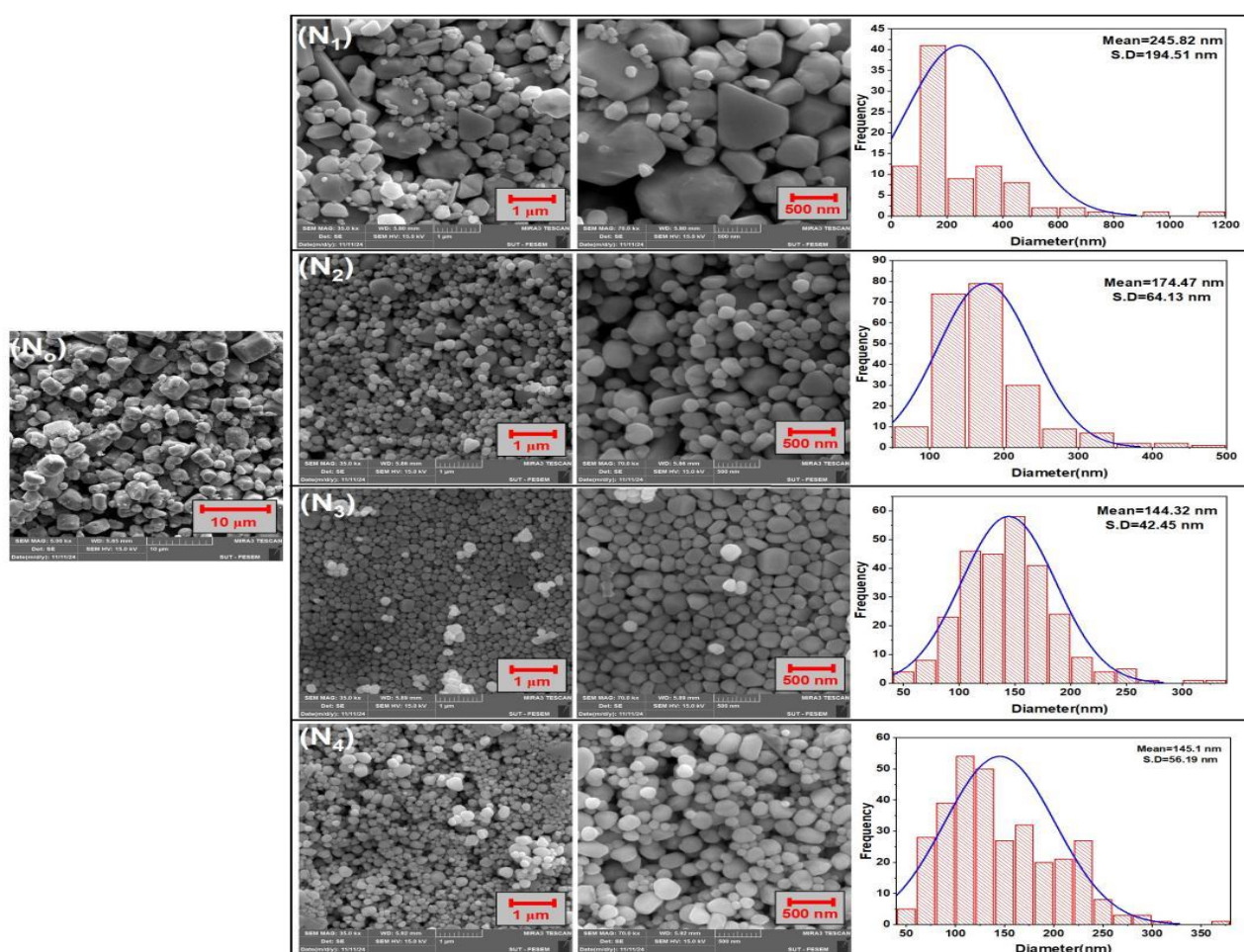


Figure 5: FESEM images with the particle diameter of the Ag NPs produced without PVP (sample N_0) and those synthesized with various amounts of PVP (0.2, 0.3, 0.4, and 0.5 mol/L) for samples N_1 , N_2 , N_3 , and N_4 , respectively.

However, the particle diameters were obtained by measuring multiple Ag NP diameters at various locations and averaging their overall sizes using the ImageJ software program.

Based on these results, it is confirmed that PVP, at an ascertained amount, speeds up the interaction between silver ions and a reducing agent.

Furthermore, visual observation of sample N₀ without PVP and sample N₃ with a concentration of 0.4 mole/L of PVP is demonstrated in Figure 6. The observable color transition from pale yellow to dark brown over time serves as evidence for the

reduction of silver ions to silver nanoparticles upon the addition of PVP. The modification in the color of the Ag NP solution results from the excitation of SPR.

The solution of sample N₀ appears to have significant sedimentation, indicating that the particles were aggregating and settling at the bottom of the vial. This suggests poor stabilization of the particles due to the absence of PVP. While the solution of sample N₃ is more homogeneous and stable, with fewer signs of sedimentation. This indicates better stabilization and dispersion of the nanoparticles in the presence of PVP.

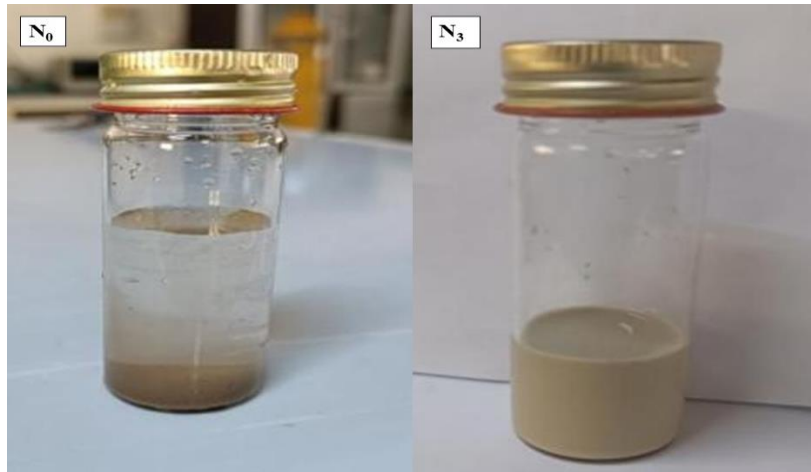


Figure 6: Ag NPs solutions procured by experiments for the sample N₀ without PVP and the sample N₃ with PVP of concentration of 0.4 mol

FTIR Spectral Analysis:

FTIR spectroscopy is commonly utilized to examine the interactions between PVP and the surfaces of Ag NPs. The investigation of functional groups capping the Ag NPs

synthesized via the hydrothermal method was investigated through FTIR spectral analysis of the samples prepared with varying concentrations of PVP (N₁, N₂, N₃, and N₄) compared with pure PVP, as shown in Figure 7.

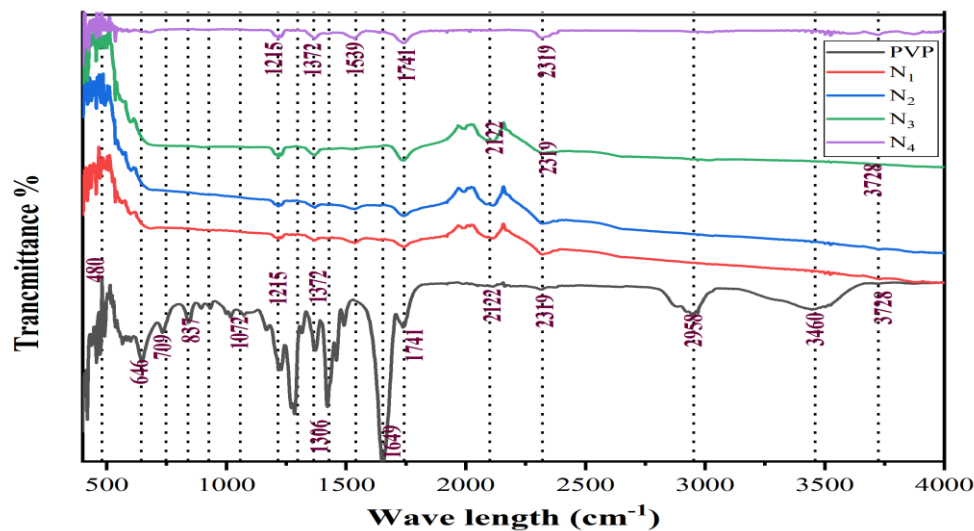


Figure 7: the FTIR spectrum of the produced Ag NPs with various amounts of PVP (0.2, 0.3, 0.4, and 0.5 mol/L) for samples N₁, N₂, N₃, and N₄ respectively, compared with the spectrum of pure PVP

FTIR research revealed the existence of many functional groups in Ag NP and pure PVP. The functional groups in pure PVP and Ag NP with PVP samples were also present, likely due to the diverse phytochemicals capping the Ag NP.

The absorbance peak in the spectrum of purified PVP, is located approximately at around 1649 cm⁻¹ attributed to the vibratory stretching of C=O in the pyrrolidone group (Oliveira *et al.*, 2022).

The significant characteristic bands at 3728 cm⁻¹ indicate the presence of water molecules or residual hydroxyl groups; the bands at about 2122 cm⁻¹ and 2319 cm⁻¹ in all samples are attributed to the O-H and N-H stretching of amides, while the band at 1741 cm⁻¹ is assigned to the C≡C stretching. Furthermore, the small bands at approximately 1539 cm⁻¹, 1372 cm⁻¹, and 1215 cm⁻¹ correspond to metal-oxygen or metal-nitrogen vibrations (Ag-O or Ag-N) and C=O stretching, observed in all samples (Slewa *et al.*, 2024).

In the peaks of pure PVP compared with peaks of PVP-Ag NPs, the alterations in the FTIR spectrum demonstrated that PVP protects Ag NPs through a coordination interaction between Ag NPs and the oxygen and nitrogen atoms of PVP. The probable interactions of the PVP molecule adsorbed onto Ag NPs include interactions solely between the outermost layer of Ag NPs and oxygen, interactions involving both oxygen and nitrogen of PVP,

4. ANTIMICROBIAL STUDY

The bactericidal efficacy of Ag NP samples prepared without PVP (N₀) and the optimal sample with PVP (N₃) was tested against two different bacterial strains, *S. aureus* and *E. coli*, using the well-diffusion technique. The antibacterial activity of Ag NP samples prepared without PVP (N₀) and the optimal sample with PVP (N₃) was tested against two different bacterial strains, *Escherichia coli* (*E. coli*) and *Staphylococcus aureus* (*S. aureus*), by using the well-diffusion technique. Fresh bacterial agriculture was prepared at 37°C for 24 h. Three wells were

and nitrogen interacting with Ag NPs. The FTIR and UV-Vis spectral analyses demonstrate that the functional groups identified in the FTIR analysis serve as the capping and reducing agents that trigger the formation of Ag NPs. Finally, the general findings of the FTIR spectra confirmed the formation of Ag NPs in the deionized water in all samples

created in the agar plate and filled with different concentrations of both samples of Ag NPs powder (0.001, 0.003, and 0.005mg/mL). Further, two other wells were also made and loaded with distilled water and antibiotic (ampicillin), which were used as negative and positive controls, respectively, as shown in Figure 8. The plates had been incubated for 24 h at 37°C. The antibacterial activity of Ag NPs on the evaluated bacterial strains was assessed by the development of an inhibition zone surrounding the wells post-incubation (Mohammed & Salih, 2022). All the antimicrobial tests were performed at the (Gagro Scientific Center in Erbil).



Figure 8: The diffusion method of wells demonstrates inhibition zones of the antibacterial activity for the samples N₀ and N₃ in different concentrations of (0.001, 0.003, and 0.005 mg/mL) against two different bacterial strains.

Different inhibition zones were found for different concentrations of Ag NPs powder. It was also found that the effect of Ag NPs is different against different types of bacteria, due to the difference in membrane structural composition of the

bacteria. The maximal diameters of the inhibition zones for various amounts of optimal Ag NPs against the two tested bacterial strains is listed in Table 2.

Table 2: Shows inhibition zones of the antibacterial activity for the samples N₀ and N₃ in different concentrations of (0.001, 0.003, and 0.005 mg/mL) against two different bacterial strains.

Pathogens	Ag NPs powder concentration (mg/mL)	Inhibition zone in(mm) of (N3)	Inhibition zone in(mm) of (N0)
<i>E. coli</i>	0.001	0	11
	0.003	0	12
	0.005	0	12
<i>S. aureus</i>	0.001	13	12
	0.003	21	13
	0.005	25	13

The results of the antibacterial activity demonstrated that all Ag NPs synthesized without PVP exhibited significant antibacterial effects against all tested bacterial strains. In contrast, Ag NPs synthesized with PVP showed enhanced antibacterial activity versus *S. aureus*, but no antibacterial activity versus *E. coli*, as indicated by the absence of a zone of inhibition on the agar plates, as illustrated in Figure 8. This may be attributed to the attraction that exists between positively charged Ag NPs and the negatively charged cell wall of *S. aureus*, which likely raised

the chance of cell-particle interactions, leading to stronger antibacterial activity. The mechanism of antibacterial activity of Ag NPs involves their ability to penetrate and disrupt bacterial membranes, particularly through smaller-sized particles, resulting in cell lysis. The discharge of silver ions (Ag⁺) from Ag NPs' surfaces is necessary for their bactericidal activity. The surface area of Ag NPs determines their ability to generate Ag⁺ ions, which can penetrate cell membranes and cause bacterial cell death (Tang & Zheng, 2018).

However, the lack of antibacterial activity in Ag NPs synthesized with PVP could be attributed to the production of a PVP layer over Ag NPs, that prevents the set free of Ag⁺, as well as the resistance of thick layers of peptidoglycans found on the cell membrane of some bacteria. At the surfaces of Ag NPs, PVP can create a thin shell that serves as a barrier between the surface and its surroundings. By obstructing active sites, PVP can also affect Ag NPs' antibacterial activity. Therefore, in order to activate Ag NPs, PVP frequently needs to be eliminated from their surfaces. Furthermore, the concentration of Ag NPs powder

has an impact on the antibacterial activity. As shown in Table 2, the findings revealed that the inhibition zone of Ag NPs against the two tested microbial strains increased with increasing the concentration of the Ag NPs powder.

Moreover, Table 3 compares the average determined particle size and maximum inhibition zone of optimal Ag NPs against the strains of the tested bacteria with some previously reported work under different conditions.

Table 3: Comparison of the average determined particle size and maximum inhibition zone of optimal Ag NPs against the strains of the tested bacteria with some previously reported work under different conditions.

Bacteria	Silver Nanoparticle Size (nm) and Shape	Maximum Inhibition Zone in (mm)	Reference
<i>S. aureus</i> <i>E. coli</i>	Spherical, 140	25 0	In this work
<i>S. aureus</i> <i>E. coli</i>	Spherical, 60	16 17	(Gao <i>et al.</i> , 2013)
<i>S. aureus</i> <i>E. coli</i>	Spherical, 27.5	21 19	(Bhatia <i>et al.</i> , 2016)

5. ROLE OF PVP ON STABILITY AND ACTIVITY OF AG NPS

The ability to preserve hydrothermal-synthesized Ag NPs for future use without modifying their characteristics is useful for various uses. The stability of Ag NPs can be determined by observing the color of the reaction solution and analyzing the spectrum of absorption. Figure 9 illustrates a comparison of the spectrum of absorption for optimal sample prepared with PVP (N₃) for fresh, after 3 months.

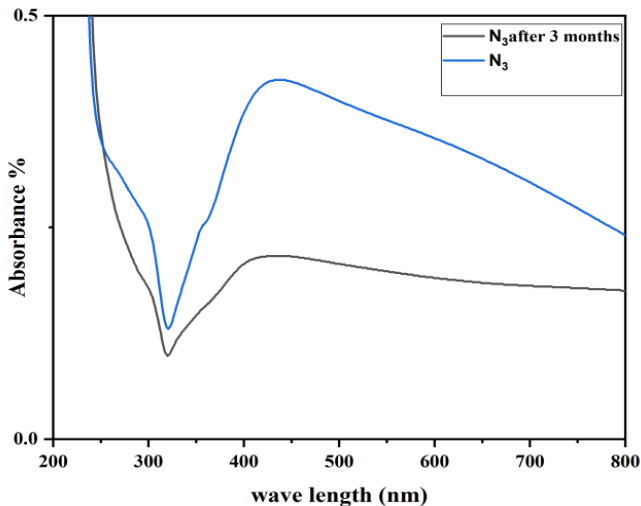


Figure 9: Absorption spectra for optimal sample prepared with PVP (N₃) for fresh, after 3 months

As seen in Figure 9, there is a small broadening of the SPR peak intensity and no discernible change in the position of the absorbance peak SPR. This indicates that PVP plays a major role in stability by preventing Ag NPs from aggregating. However, a slight decrease in the SPR peak intensity with slightly broadening may be due to the ambient conditions of storing the sample such as heat and light which affected on their properties. The stability of synthesized nanoparticles for 3 months confirmed that they can be used for a long time after preparation. In addition to shape and surface charge, nanoparticle size determines the stability and sustained antibacterial activity of Ag NPs. Nanoparticles with high activity are best suited for short-term applications, but those

with low activity can be used for longer periods of time, depending on the purpose. Ag NPs of smaller sizes demonstrated greater antibacterial activity because of (Mirzaei *et al.*, 2017; Zein *et al.*, 2022):

1) Smaller Ag NPs via a higher surface-to-volume ratio have more contact areas with bacteria's cell walls; 2) Smaller Ag NPs set free more ions at a faster rate than larger Ag NPs; and 3) Smaller Ag NPs can penetrate cell walls, causing additional damage to the cells by emitting Ag ions within them.

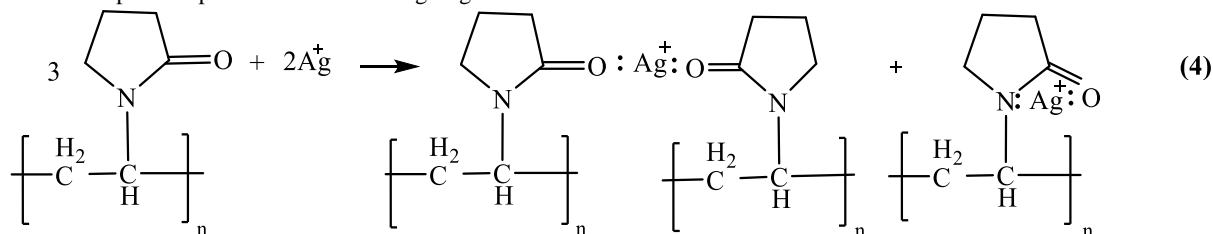
Stabilizing agents are often applied to Ag NPs to improve their stability and protect their activities. PVP is one of the most popular capping agents for Ag NPs. The high surface area-to-volume ratio of Ag NPs leads to their increased reactivity, which can cause particle aggregation and settling; Therefore, a capping agent is required to guarantee colloidal stability by mechanisms such as electrostatic or steric repulsion. A capping agent can be used to stabilize particles and prevent them from aggregating. Additionally, a stabilizer can dramatically boost the antibacterial activity of Ag NPs by preventing the particles from aggregating. The impact of PVP on the formation and properties of the resulting Ag NPs was investigated by producing precursor mixtures containing various PVP: Ag molar ratios.

A low stabilizer concentration leads to the synthesis of primarily nanoscale Ag NPs, as well as a few bigger clusters. In this situation, the silver atoms fail to make adequate coordination bonds with the stabilizer, forcing them to consolidate and form bigger agglomerates. The creation of homogeneous nanosized particles is not possible with the little amount of stabilizer. The particle size distribution is unaffected significantly by the rising PVP concentration, however more clusters are created. The formation of a dense polymeric network at high stabilizer concentrations makes it difficult to observe the nanostructures. Furthermore, an excessive amount of stabilizer can hinder the nanoparticles' interactions with other molecules by entangling them in the thick stabilizer network (Gharibshahi *et al.*, 2017; Van Viet *et al.*, 2018).

Interestingly, PVP can operate as a barrier between the Ag NPs surface and its surroundings by forming a very thin shell (1 to 2) nm at the Ag NPs surfaces. By obstructing active sites, PVP can also affect Ag NPs' catalytic activity. Therefore, in order to permit certain applications, PVP frequently needs to be removed from Ag NPs surfaces. The Ag NPs' shape is unaltered and their catalytic activity is increased upon removal. PVP can be eliminated to solve this problem by using heat or H₂O₂/H₂SO₄ treatments (El Amri & Roger, 2020).

Noteworthy, the role of PVP for producing stable Ag NP is attributable to: 1) modifies the nucleation extension of nanoparticles, which is influenced by the PVP concentration; 2) limits nanoparticle accumulation; 3) enhances the degree of crystal structure in the nanoparticles; and 4) it facilitates particle growth by a uniform distribution of size and morphology (Koczur *et al.*, 2015).

The creation of coordination bonds between PVP and silver ions is an important process for stabilizing Ag NPs. This



Finally, Ag NPs exhibit significant toxicity towards microorganisms, including bacteria; hence, they are extensively utilized as antibacterial agents in medical devices and consumer products. However, controlling the particle size of Ag NPs is critical, as prior research has demonstrated that their bactericidal efficacy is size-dependent, with smaller particles having stronger antibacterial activity. Furthermore, the stability of Ag NPs can have a major impact on the long-term efficacy of their antibacterial actions. Consequently, this study aims to synthesize ultra-fine Ag NPs by hydrothermal route and used it on some selected bacteria to determine their effectiveness.

The novelty of the research may be identified in two main aspects: the first is the synthesis of Ag NPs using pure AgNO₃ powder immersed in deionized water with the aid of PVP used as a stabilizing agent, the second is stabilized Ag NPs with low concentrations exhibited excellent antibacterial efficiency against bacteria strains, the small nanoscale dimensions of Ag NPs, characterized by a spherical morphology, constitute the optimal size and appropriate shape requisite for antibacterial efficacy. It can be said that Ag NPs affect the bacteria's structure and diminish its activity. These properties make Ag NPs appropriate for their usage in the biomedical fields where they might be used to kill some types of bacteria or inhibit them competently. This demonstrates that Ag NPs can be an alternative to antibiotics drugs in the future.

CONCLUSION

This work presents the synthesis of Ag NPs by hydrothermal technique using PVP as a stabilizing agent. The study aimed to control the morphology and particle size distribution of the synthesized Ag NPs, which in turn increased their chemical activity surface area. The morphology, structure, and optical properties of synthesized Ag NPs were characterized by UV-vis absorption spectroscopy, XRD, FESEM, and FTIR. Their antibacterial activity was evaluated against Gram-negative and Gram-positive bacterial strains by the well diffusion method.

The results indicated that adding PVP during the synthesis process diminishes the size of Ag NPs and yields more stable nanoparticles compared to those synthesis without PVP, due to the capping effect of PVP, which stabilizes the Ag NPs against aggregation. The calculated values of E_g from the absorption peaks of the UV/Vis- spectra was found to be increased from 1.70 eV to 1.87 eV with increasing the concentration of PVP from 0.2 mol/L to 0.5 mol/L. The average size of the optimized Ag NPs that were captured in FESEM was found to be in the range of 140 nm. It has been found that Ag NPs synthesized without addition of PVP positively affects the antibacterial properties of Ag NPs. Showed significant antibacterial activity towards the tested bacteria, with maximum inhibition of 12 mm for gram-negative and 13 mm for gram-positive. Ag NPs synthesized with addition of PVP showed no inhibition towards gram-negative bacteria but

connection enables PVP to control nanoparticle development, inhibit aggregation, and improve stability, making it an important capping and stabilizing agent in nanomaterial fabrication. In PVP's carbonyl (-C=O) group, the oxygen atom has a single pair of electrons. The silver ion (Ag⁺), which functions as an electron acceptor, receives this lone pair. Consequently, as the reaction scheme (Eq.4) shows, a PVP-Ag⁺ coordination complex is created (Ding *et al.*, 2012; Perumal *et al.*, 2017):

had inhibitory activity towards gram-positive with maximum inhibition zone of 25 mm. The optimal synthesized PVP-Ag NPs were found to be nearly stable for 3 months, so it can maintain its efficiency for a period after preparation and used for the required purposes.

Acknowledgments:

The author would like to sincerely acknowledge and thank the Physics and Chemistry Departments at the College of Science, Salahaddin University, for their invaluable assistance and for providing the necessary equipment and materials to complete this research.

Ethical Statement :

The current experiment was approved by the Ethical Committee of the College of Science at the University of Salahaddin in Erbil, Kurdistan Region.

Author Contributions:

All authors have reviewed the final version to be published and agreed to be accountable for all aspects of the work.

REFERENCES

- Abbas, R., Luo, J., Qi, X., Naz, A., Khan, I. A., Liu, H., Yu, S., & Wei, J. (2024). Silver nanoparticles: Synthesis, structure, properties and applications. *Nanomaterials*, 14(17), 1425. <https://doi.org/https://doi.org/10.3390/nano14171425>
- Ahmad, A. A. (2022). Solid State Synthesis of Silver Nanoparticles Using Violuric Acid as a Novel Reducing Agent. *Science Journal of University of Zakho*, 10(4), 193-196. <https://doi.org/https://doi.org/10.25271/sjuoz.2022.10.4.1021>
- Altammar, K. A. (2023). A review on nanoparticles: characteristics, synthesis, applications, and challenges. *Frontiers in microbiology*, 14, 1155622. <https://doi.org/https://doi.org/10.3389/fmicb.2023.1155622>
- Bamiduro, F., William, N., Hondow, N., Milne, S., Nelson, A., & Drummond-Brydson, R. (2018). Hydrothermal Synthesis of Silver Nanoparticles for High Throughput Biosensing Applications. *MRS Advances*, 3(15-16), 861-866. <https://doi.org/https://doi.org/10.1557/adv.2018.197>
- Bhatia, D., Mittal, A., & Malik, D. K. (2016). Antimicrobial activity of PVP coated silver nanoparticles synthesized by Lysinibacillus varians. *3 Biotech*, 6, 1-8. <https://doi.org/https://doi.org/10.1007/s13205-016-0514-7>

- Cheng, Y., Wang, M., Fang, C., Wei, Y., Chen, J., & Zhang, J. (2021). Variability and improvement of optical and antimicrobial performances for QCDs/mesoporous SiO₂/Ag NPs composites via in situ synthesis. *Green Processing and Synthesis*, 10(1), 403-411. <https://doi.org/https://doi.org/10.1515/gps-2021-0035>
- Dakal, T. C., Kumar, A., Majumdar, R. S., & Yadav, V. (2016). Mechanistic basis of antimicrobial actions of silver nanoparticles. *Frontiers in microbiology*, 7, 1831. <https://doi.org/https://doi.org/10.3389/fmicb.2016.01831>
- Ding, X., Kan, C., Mo, B., Ke, S., Cong, B., Xu, L., & Zhu, J. (2012). Synthesis of polyhedral Ag nanostructures by a PVP-assisted hydrothermal method. *Journal of Nanoparticle Research*, 14, 1-9. <https://doi.org/https://doi.org/10.1007/s11051-012-1000-8>
- Duman, H., Eker, F., Akdaşçi, E., Witkowska, A. M., Bechelany, M., & Karav, S. (2024). Silver nanoparticles: A comprehensive review of synthesis methods and chemical and physical properties. *Nanomaterials*, 14(18), 1527. <https://doi.org/https://doi.org/10.3390/nano14181527>
- Eker, F., Duman, H., Akdaşçi, E., Bolat, E., Sarıtaş, S., Karav, S., & Witkowska, A. M. (2024). A comprehensive review of nanoparticles: from classification to application and toxicity. *Molecules*, 29(15), 3482. <https://doi.org/https://doi.org/10.3390/molecules29153482>
- El Amri, N., & Roger, K. (2020). Polyvinylpyrrolidone (PVP) impurities drastically impact the outcome of nanoparticle syntheses. *Journal of Colloid and Interface Science*, 576, 435-443. <https://doi.org/https://doi.org/10.1016/j.jcis.2020.04.113>
- Esmael, M. M. (2024). ENHANCED SYNTHESIS OF NiO NANO FILM THROUGH SOL-GEL DIP COATING METHOD: INVESTIGATION THE IMPACT OF LASER IRRADIATION. *Science Journal of University of Zakho*, 12(4), 436-441. <https://doi.org/https://doi.org/10.25271/sjuoz.2024.12.4.1308>
- Feng, S.-H., & Li, G.-H. (2017). Hydrothermal and solvothermal syntheses. In *Modern inorganic synthetic chemistry* (pp. 73-104). Elsevier. <https://doi.org/https://doi.org/10.1016/B978-0-444-63591-4.00004-5>
- Ferreira, A. M., Vikulina, A., Loughlin, M., & Volodkin, D. (2023). How similar is the antibacterial activity of silver nanoparticles coated with different capping agents? *RSC advances*, 13(16), 10542-10555. <https://doi.org/DOI:10.1039/D3RA00917C>
- Gao, M., Sun, L., Wang, Z., & Zhao, Y. (2013). Controlled synthesis of Ag nanoparticles with different morphologies and their antibacterial properties. *Materials Science and Engineering: C*, 33(1), 397-404. <https://doi.org/https://doi.org/10.1016/j.msec.2012.09.05>
- Ghadiri, M., Hallajzadeh, J., Akhghari, Z., Nikkhah, E., & Othman, H. (2023). Green synthesis and antibacterial effects of silver nanoparticles on novel activated carbon. *Iran J. Chem. Chem. Eng.*
- Gharibshahi, L., Saion, E., Gharibshahi, E., Shaari, A. H., & Matori, K. A. (2017). Influence of Poly (vinylpyrrolidone) concentration on properties of silver nanoparticles manufactured by modified thermal treatment method. *PLoS One*, 12(10), e0186094. <https://doi.org/https://doi.org/10.1371/journal.pone.0186094>
- Ivlieva, A., Petritskaya, E., Rogatkin, D., Yushin, N., Grozdov, D., Vergel, K., & Zimicovskaia, I. (2022). Does nanosilver have a pronounced toxic effect on humans? *Applied Sciences*, 12(7), 3476. <https://doi.org/https://doi.org/10.3390/app12073476>
- Jalal, V. J. (2024). Structural and optical properties of polymer blend nanocomposites based on PVP/PVA incorporated AgNO₃. *Journal of Physics Communications*, 8(5), 055004. <https://doi.org/DOI.10.1088/2399-6528/ad4e97>
- Khan, I., Saeed, K., & Khan, I. (2019). Nanoparticles: Properties, applications and toxicities. *Arabian journal of chemistry*, 12(7), 908-931. <https://doi.org/https://doi.org/10.1016/j.arabj.2017.05.011>
- Khizir, H. A., & Abbas, T. A.-H. (2021). Hydrothermal growth and controllable synthesis of flower-shaped TiO₂ nanorods on FTO coated glass. *Journal of Sol-Gel Science and Technology*, 98, 487-496. <https://doi.org/https://doi.org/10.1007/s10971-021-05531-z>
- Koczur, K. M., Mourdikoudis, S., Polavarapu, L., & Skrabalak, S. E. (2015). Polyvinylpyrrolidone (PVP) in nanoparticle synthesis. *Dalton transactions*, 44(41), 17883-17905. <https://doi.org/https://doi.org/10.1039/C5DT02964C>
- Li, J., Wu, Q., & Wu, J. (2016). Synthesis of nanoparticles via solvothermal and hydrothermal methods. 12. In: Springer international publishing Switzerland.
- Liu, H., Wang, S., Li, Z., Zhuo, R., Zhao, J., Duan, Y., Liu, L., & Yang, J. (2024). Experimental study on the preparation of monodisperse nano-silver by hydrothermal synthesis. *Materials Chemistry and Physics*, 314, 128902. <https://doi.org/https://doi.org/10.1016/j.matchemphys.2024.128902>
- Mirzaei, A., Janghorban, K., Hashemi, B., Bonyani, M., Leonardi, S. G., & Neri, G. (2017). Characterization and optical studies of PVP-capped silver nanoparticles. *Journal of Nanostructure in Chemistry*, 7, 37-46. <https://doi.org/https://doi.org/10.1007/s40097-016-0212-3>
- Mohammed, J. H., & Salih, N. A. M. (2022). Synthesis and characterization of some new nitrones derivatives and screening their biological activities. *Science Journal of University of Zakho*, 10(4), 268-273. <https://doi.org/https://doi.org/10.25271/sjuoz.2022.10.4.1096>
- More, P. R., Pandit, S., Filippis, A. D., Franci, G., Mijakovic, I., & Galdiero, M. (2023). Silver nanoparticles: bactericidal and mechanistic approach against drug resistant pathogens. *Microorganisms*, 11(2), 369. <https://doi.org/https://doi.org/10.3390/microorganisms11020369>
- Neto, F. N. S., Morais, L. A., Gorup, L. F., Ribeiro, L. S., Martins, T. J., Hosida, T. Y., Francatto, P., Barbosa, D. B., Camargo, E. R., & Delbem, A. C. (2023). Facile synthesis of PVP-Coated silver nanoparticles and evaluation of their physicochemical, antimicrobial and toxic activity. *Colloids and Interfaces*, 7(4), 66. <https://doi.org/https://doi.org/10.3390/colloids7040066>
- Obaidallah, J., & Ahmed, S. A. (2023). CHARACTERIZATION OF SYNTHESIZED SILVER NANOPARTICLES USING LEPIDIUM SATIVUM PLANT. *Science Journal of University of Zakho*, 11(4), 548-556-548-556. <https://doi.org/https://doi.org/10.25271/sjuoz.2023.11.4.1174>
- Oliveira, A. E. F., Pereira, A. C., de Resende, M. A. C., & Ferreira, L. F. (2022). Synthesis of a silver nanoparticle ink for fabrication of reference electrodes. *Talanta Open*, 5, 100085. <https://doi.org/https://doi.org/10.1016/j.talo.2022.100085>
- Perumal, R., Casale, S., De Stefano, L., & Spadavecchia, J. (2017). Synthesis and characterization of Ag-Protoporphyrin nano structures using mixed co-polymer

- method. *Frontiers in Laboratory Medicine*, 1(2), 49-54. <https://doi.org/https://doi.org/10.1016/j.flm.2017.05.002>
- Slewa, L. H., Abbas, T. A., & Ahmed, N. M. (2019). Hydrothermal and solvothermal synthesis of nanorods and 3D (micro/nano) V₂O₅ on macro PSi substrate for pH-EGFET sensors. *Journal of Materials Science: Materials in Electronics*, 30, 11193-11207. <https://doi.org/https://doi.org/10.1007/s10854-019-01465-z>
- Slewa, L. H., Gozeh, B. A., Ismael, D. S., FageAbdulla, N. Q., & Othman, H. O. (2024). Antibacterial and Antifungal Activity of Ag-NPs Colloids Prepared by a Hydrothermal Reaction in Green Synthesized CQD. *BioNanoScience*, 1-17. <https://doi.org/https://doi.org/10.1007/s12668-024-01486-x>
- Tang, S., & Zheng, J. (2018). Antibacterial activity of silver nanoparticles: structural effects. *Advanced healthcare materials*, 7(13), 1701503. <https://doi.org/https://doi.org/10.1002/adhm.201701503>
- Tooklang, P., Audtarat, S., Chaisen, K., Thepsiri, J., Chingsungnoen, A., Jittabut, P., & Dasri, T. (2024). Functionalization of silver nanoparticles coating cotton fabrics through hydrothermal synthesis for improved antimicrobial properties. *Nano Express*, 5(2), 025009. <https://doi.org/DOI 10.1088/2632-959X/ad437b>
- Van Viet, P., Sang, T. T., Bich, N. H. N., & Thi, C. M. (2018). An improved green synthesis method and Escherichia coli antibacterial activity of silver nanoparticles. *Journal of Photochemistry and Photobiology B: Biology*, 182, 108-114. <https://doi.org/https://doi.org/10.1016/j.jphotobiol.2018.04.002>
- Wang, J., Yu, Y., Zhao, X., Sun, J., Wang, Y., & Zhu, H. (2023). A review on the size-dependent bulking, vibration and wave propagation of nanostructures. *Journal of Physics: Condensed Matter*, 35(29), 293001. <https://doi.org/DOI 10.1088/1361-648X/acc62b>
- Yaqoob, A. A., Umar, K., & Ibrahim, M. N. M. (2020). Silver nanoparticles: various methods of synthesis, size affecting factors and their potential applications—a review. *Applied Nanoscience*, 10(5), 1369-1378. <https://doi.org/https://doi.org/10.1007/s13204-020-01318-w>
- Yatem, A. A., & Rammoo, M. S. (2023). Nanostructured Silver Thin Film: Using Successive Ionic Layer Adsorption and Reduction Method. *Science Journal of University of Zakho*, 11(1), 73-77. <https://doi.org/https://doi.org/10.25271/sjuoz.2023.11.1.1017>
- Zein, R., Alghoraibi, I., Soukkarieh, C., Ismail, M. T., & Alahmad, A. (2022). Influence of polyvinylpyrrolidone concentration on properties and anti-bacterial activity of green synthesized silver nanoparticles. *Micromachines*, 13(5), 777. <https://doi.org/https://doi.org/10.3390/mi13050777>